Contributing Factors Concerning Inconsistencies in Persistent Atrial Fibrillation Ablation Outcomes

Tiago P Almeida[1], Gavin S Chu[1,2], Xin Li[1], João L Salinet[3], Nawshin Dastagir[1], Michael J Bell[1], Frederique J Vanheusden[4], Jiun H Tuan[2], Peter J Stafford[2], G A Ng[1,2], Fernando S Schlindwein[1]

[1]University of Leicester, UK
[2]University Hospitals of Leicester NHS Trust, UK
[3]Federal ABC University and Heart Institute (InCor), Brazil
[4]University of Southampton, Southampton, United Kingdom

Abstract

In the present work, we investigated current methods for complex fractionated atrial electrogram (CFAE) classification during persistent atrial fibrillation (persAF). Potential contributing factors concerning the low reproducibility of CFAE-guided ablation outcomes in persAF therapy have been explored, such as inconsistencies in automated CFAE classification performed by different systems, the co-existence of different types of atrial electrograms (AEGs), and insufficient AEG duration for CFAE detection. First, we show that CFAE classification may vary for the same individual, depending on the system being used and settings being applied. Revised thresholds are suggested for the indices calculated by each system to minimize the differences in CFAE detection performed independently by them. Second, our results show that some AEGs are affected by stepwise persAF ablation, while others remain unaffected by it. Different types of AEGs might correlate with distinct underlying persAF mechanisms. Single descriptors measured from the AEGs, such as sample entropy and dominant frequency, were not able to discriminate the different types of AEGs individually, but multivariate analysis using multiple descriptors measured from the AEGs can effectively discriminate the different types of AEGs. Finally, we show that AEG duration of 2.5 s – as currently used by some systems – might not be sufficient to measure CFAEs consistently.

1. Introduction

Atrial fibrillation (AF) is the most common sustained cardiac arrhythmia found in clinical practice, characterized by irregular atrial mechanical function, and it is a leading cause of stroke [1]. Although pulmonary vein isolation (PVI) has been proved effective in treating paroxysmal AF, the identification of critical areas for successful ablation in patients with persistent AF (persAF) remains a challenge due to an incomplete understanding of the underlying pathophysiology of the arrhythmia [1]. Complex fractionated atrial electrograms (CFAEs) are believed to represent remodeled atrial substrate and are, therefore, potential targets for persAF ablation [2]. CFAE ablation has been accepted as an additional therapy to PVI to treat persAF. Inconsistent CFAE-guided ablation outcomes have, however, cast doubt on the efficacy of this approach [3]. Currently, clinical studies rely on automated CFAE classification performed by algorithms embedded in commercial mapping systems to identify CFAEs during persAF ablation. Different companies have developed algorithms based on different features of the atrial electrogram (AEG). Inconsistencies between these algorithms could lead to discordant CFAE classifications by the available systems [4]. Additionally, while studies support that some CFAEs truly represent local AF drivers, others suggest CFAEs are resultant from distant AF drivers [5,6]. Finally, the spatio-temporal behavior of AEGs in persAF remains contentious [7]. We hypothesized that these factors might contribute to disparities in ablation target identification based on AEG fractionation in persAF. This study investigated factors that directly influence the low reproducibility of CFAE-guided ablation outcomes in persAF therapy, such as inconsistencies in automated CFAE classification, the co-existence of different types of AEGs, and insufficient AEG duration for CFAE detection.

2. Materials and methods

The study population consisted of 18 persAF patients (16 male; mean age 56.1 ± 9.3 years; history of AF 67.2 ± 45.6 months) referred to our institution for first time catheter ablation [6]. Study approval was obtained from the local ethics committee and all procedures were performed with full informed consent. 3D left atrial (LA)

geometry was created using Ensite NavX™ (St. Jude Medical, St. Paul, Minnesota). PVI was performed followed by the creation of linear roof lines (PVI+RL) using a deflectable, variable loop circular mapping catheter (Inquiry Optima, St. Jude Medical). Bipolar AEGs were collected from 15 pre-determined atrial regions before and after LA ablation for each patient [6]. 797 AEGs (455 before and 342 after PVI+RL) were recorded from the LA (sampling frequency 1.2 kHz) and band-pass filtered (30 – 300 Hz).

2.1. Automated CFAE classification

The two commercial systems most frequently used in clinical practice are the NavX and the CARTO (Biosense Webster, Diamond Bar, California) [4]. Those systems provide primary indices to assess CFAE objectively [NavX: CFE-Mean; CARTO: Interval Confidence Level (ICL)], and complementary indices to further support the electrophysiology procedure [NavX: CFE-StdDev; CARTO: Average Complex Interval (ACI), Shortest Complex Interval (SCI)]. There are no defined recommended thresholds for the complementary indices to characterize CFAEs. To compare both systems, the 797 AEGs with their respective CFE-Mean and CFE-StdDev were exported from NavX. The ICL, ACI and SCI, as defined by CARTO, were calculated offline with a validated (100% agreement) MATLAB algorithm [4]. CFAE classification was performed by NavX and CARTO using their default clinical thresholds (CFE-Mean $\leq$ 120 ms; ICL $\geq$ 7) [8]. Primary and complementary indices from each system were optimized to reduce the differences in CFAE detection between them using receiver operating characteristic (ROC) curves. The agreement between both systems was assessed with Cohen's kappa (κ) [9].

2.2. Different types of AEGs

From the 797 AEGs, 207 pairs were identified as collected from corresponding LA regions: 207 before and 207 after PVI+RL. Nine descriptors were measured from the 207 pairs of AEGs, accordingly: CFE-Mean, CFE-StdDev, ICL, ACI, SCI [4], sample entropy (SampEn) [10], peak-to-peak (PP) [11], dominant frequency (DF) [12] and organization index (OI) [13]. Multivariate analysis of variance (MANOVA) and linear discriminant analysis (LDA) were used to test the differences between the AEGs before and after PVI+RL using all descriptors. CFAEs were defined as CFE-Mean $\leq$ 84 ms; ICL $\geq$ 4.

2.3. AEG duration for CFAE detection

Previous work has investigated different segment lengths to consistently characterize CFAEs using NavX, since this system allows for different AEG duration recordings (1 s to 8 s) [7]. CARTO, however inherently limits the AEG collection to 2.5 s, hampering the investigation of CFAE temporal behavior using this system. To overcome this limitation, consecutive 2.5 s AEG segments were assessed to infer about temporal consistency of AEG. CFAE classifications performed in AEGs with different segment lengths have been analyzed to search for the 'optimum' length of AEGs needed for identification of CFAEs. Accordingly, the 797 bipolar AEGs were exported from NavX with three segment lengths (2.5 s, 5 s and 8 s). The AEGs with 8 s duration were divided into three consecutive 2.5 s segments. CARTO's criterion for CFAE classification (ICL, ACI and SCI) was applied offline to all cases.

2.4. Statistical analysis

Nonparametric paired multiple data were analyzed using the Friedman test with Dunn's correction. Nonparametric unpaired data were analyzed using the Mann–Whitney test. Categorical data were expressed as percentages and analyzed using the two-sided Yates-corrected Chi-square test. $P \leq 0.05$ was considered statistically significant.

3. Results

3.1. Automated CFAE classification

The CFAE classifications performed by NavX and CARTO with their respective default thresholds for CFAE detection (CFE-Mean $\leq$ 120 ms, ICL $\geq$ 7, respectively) do not always agree (Figure 1A).

Initially assuming CFE-Mean $\leq$ 120 ms as the reference for CFAE classification, the default threshold for CARTO (ICL $\geq$ 7) provides high specificity but poor sensitivity for CFAE detection (Table 1, Figure 1B). The optimum threshold found from the ROC curves (ICL $\geq$ 4) provides optimum sensitivity and specificity for CFAE detection and classification when using NavX as the comparator. Now, assuming ICL $\geq$ 7 as the reference for CFAE classification, the default threshold for NavX (CFE-Mean $\leq$ 120 ms) provides high sensitivity but poor specificity for CFAE detection (Table 1, Figure 1C). CFE-Mean $\leq$ 84 ms provides optimum sensitivity and specificity for CFAE detection and classification when using CARTO as the comparator. The results from the ROC curves suggest that CFE-StdDev $\leq$ 47 ms, ACI $\leq$ 82 ms and SCI $\leq$ 58 ms provide optimum sensitivity and specificity for CFAE detection, when considering the agreement between CFE-Mean and ICL for CFAE classification (Table 1, ROC curves omitted). Using the default thresholds NavX classified 69±5% of the AEGs as CFAEs, while CARTO detected 35±5% ($P<0.0001$).

Table 1. Threshold optimization for ICL, CFE-Mean, CFE-StdDev, ACI and SCI.

Classifier	Thresholds	Sensitivity	1-Specificity	AUROC	P-Value
CFE-Mean ≤ 120 ms	$ICL_{Default} \geq 7$	0.492±0.008	0.050±0.005	0.852±0.005	****
	$ICL_{Revised} \geq 3.8±0.4$	0.777±0.022	0.162±0.022		
ICL ≥ 7	$CFE\text{-}Mean_{Default} \leq 120$ ms	0.958±0.005	0.552±0.009	0.755±0.005	****
	$CFE\text{-}Mean_{Revised} \leq 84.1±0.4$ ms	0.807±0.010	0.362±0.006		
CFE-Mean ≤ 84 & ICL ≥ 4	CFE-StdDev ≤ 46.6±0.8 ms	0.905±0.012	0.185±0.008	0.877±0.014	****
CFE-Mean ≤ 84 & ICL ≥ 4	ACI ≤ 82.2±0.3 ms	0.827±0.010	0.360±0.009	0.759±0.006	****
CFE-Mean ≤ 84 & ICL ≥ 4	SCI ≤ 58.6±0.4 ms	0.816±0.012	0.300±0.009	0.812±0.005	****

AUROC = Area under ROC curve. Values in mean (±SD). **** P<0.0001.

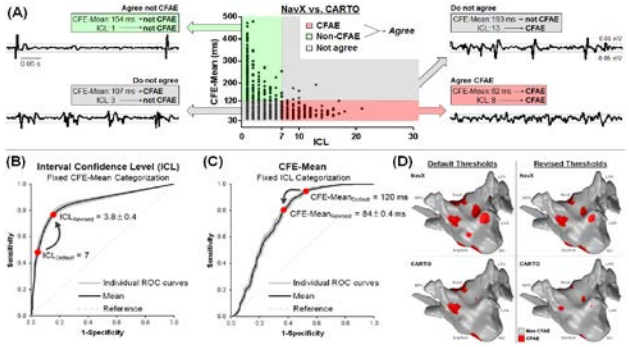

Figure 1: (A) Comparison of CFAE classifications performed by CFE-Mean and ICL for all AEGs. ROC curves and threshold customization for ICL (B) and CFE-Mean (C). (D) CFAE maps (LA anterior view) performed by NavX (upper) and CARTO (bottom) using their default (left) and revised (right) thresholds [4].

With the revised thresholds, NavX classified 45±4%, while CARTO detected 42±5% (P<0.0001). Kappa score between the CFAE categorization performed by NavX and CARTO significantly increased (P<0.0001) from 0.34±0.07 (marginal agreement, P<0.0001) using their default thresholds to 0.45±0.10 (good agreement, P<0.0001) with the revised thresholds, resulting in more similar CFAE maps (Figure 1D).

3.2. Different types of AEGs

At baseline, 70% of the AEGs were classified as CFAEs, while 40% were classified as CFAEs after PVI+RL (P<0.0001). Four groups of AEGs were distinguished in terms of the presence of fractionation before and after PVI+RL (Figure 2): 45% of the AEGs that were CFAE before ablation remained CFAE after ablation (G1), while 55% converted to non-CFAE (G2); 29% of the non-CFAE prior to ablation became CFAE (G3), while 71% remained non-CFAE (G4). The descriptors showed poor correlation with each other (Spearman's correlation, ρ; Figure 3), but were significantly affected by PVI+RL. MANOVA suggests a significant main effect of the groups of AEGs (1, 2, 3 and 4) on the descriptors on both before (F-ratio F = 12, P<0.0001) and after ablation (F = 17, P<0.0001) datasets. LDA revealed three discriminant functions both before and after ablation. Prior to any ablation, LDA successfully discriminated 62% of the AEGs in group 1; 70% of group 2; 50% of group 3 and; 64% of group 4. After PVI+RL, LDA improved, discriminating 97% of the AEGs in group 1; 83% of group 2; 5.6% of group 3 and; 46% of group 4.

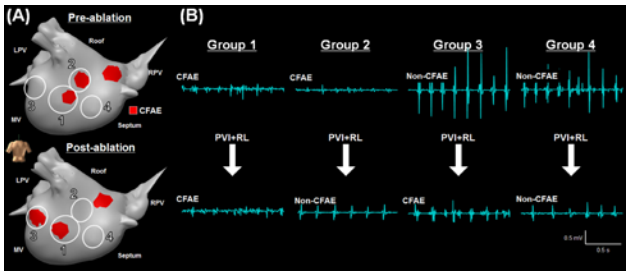

Figure 2: (A) CFAE maps before and after PVI+RL. (B) Illustration of the different types of AEGs.

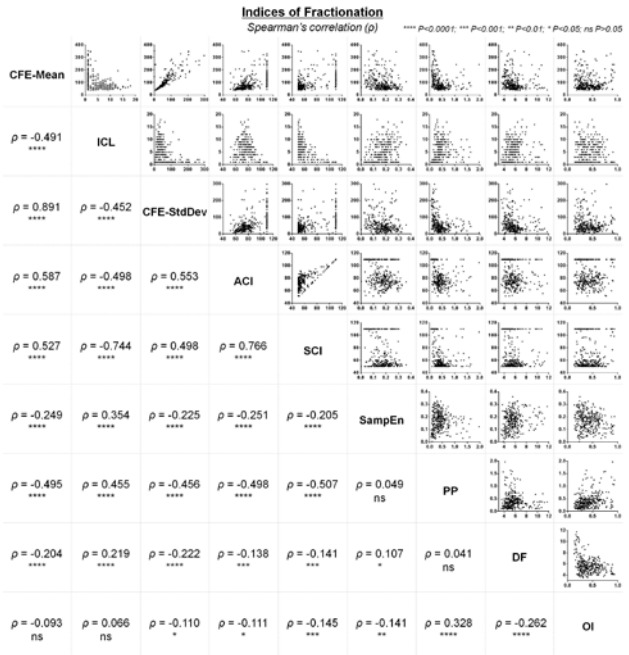

Figure 3: Correlations between different descriptors measured from the same AEG database.

3.3. AEG duration for CFAE detection

Three types of AEGs have been identified when investigating the consecutive segments with the CARTO criteria: 'stable CFAEs' as AEGs with ICL ≥ 4 in all assessed segments; 'stable non-CFAEs' as AEGs with ICL < 4 in all assessed segments and; 'unstable AEG' as AEGs with ICL varying to and from ICL ≥ 4 to ICL < 4. A total of 43% AEGs were stable CFAEs, 27% were stable non-CFAEs, while nearly 30% were unstable AEGs. AEG classification within the consecutive segments had moderate correlation (segment 1 vs 2: ρ=0.74, κ=0.62; segment 1 vs 3: ρ=0.73; κ=0.62; segment 2 vs 3: ρ=0.75; κ=0.68), and different AEG segment resulted in different CFAE maps (Figure 4A). AEGs with 5 s generated AEG classification more similar to 8 s (ρ=0.96; κ=0.87) than 2.5 s vs 5 s (ρ=0.93; κ=0.84) and 2.5 s vs 8 s (ρ=0.90; κ=0.78) (Figure 4B).

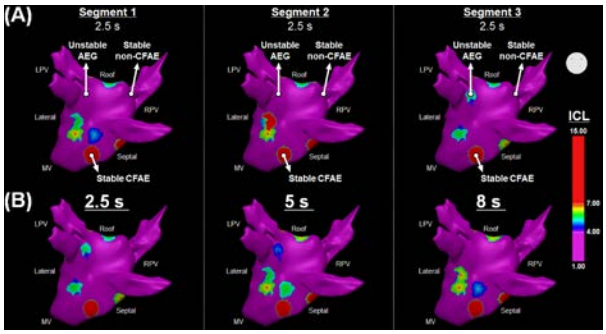

Figure 4: CFAE maps for the consecutive AEG segments (A) and for the different segment lengths (B).

4. Discussion and conclusion

Despite many efforts, the current form of CFAE-guided ablation has failed to provide a definite solution for persAF therapy [3]. Differences in existing methods for automated atrial substrate identification [4], and insufficient understanding of the underlying mechanisms involved in AF initiation and perpetuation [5] are contributing factors to inconsistencies in patient-specific persAF ablation [4]. Indeed not all AEG fractionation might represent AF drivers, but some fractionated AEGs are surrogates of critical sites for AF maintenance, and better characterization of these may result in better outcomes in persAF ablation. CFAE-guided ablation is, and for now will continue to be, an important procedure in the treatment of AF. However, a thorough re-evaluation of the definition of CFAE is necessary in order to refine the identification of atrial regions responsible for the perpetuation of persAF.

Acknowledgements

To Leicester NIHR Cardiovascular Biomedical Research Unit, UK, and the Conselho Nacional de Desenvolvimento Científico e Tecnológico, Brazil.

References

[1] Oral H, Knight BP, Tada H, Ozaydin M, Chugh A, Hassan S, et al. Pulmonary vein isolation for paroxysmal and persistent atrial fibrillation. Circulation 2002;105:1077-1081.

[2] Nademanee K, McKenzie J, Kosar E, Schwab M, Sunsaneewitayakul B, Vasavakul T, et al. A new approach for catheter ablation of atrial fibrillation: Mapping of the electrophysiologic substrate. J Am Coll Cardiol 2004;43:2044-2053.

[3] Verma A, Jiang CY, Betts TR, Chen J, Deisenhofer I, Mantovan R, et al. Approaches to catheter ablation for persistent atrial fibrillation. N Engl J Med 2015;372:1812-1822.

[4] Almeida TP, Chu GS, Salinet JL, Vanheusden FJ, Li X, Tuan JH, et al. Minimizing discordances in automated classification of fractionated electrograms in human persistent atrial fibrillation. Med Biol Eng Comput 2016;published online 25 February 2016:1-12.

[5] Takahashi Y, O'Neill MD, Hocini M, Dubois R, Matsuo S, Knecht S, et al. Characterization of electrograms associated with termination of chronic atrial fibrillation by catheter ablation. J Am Coll Cardiol 2008;51:1003-1010.

[6] Tuan J, Jeilan M, Kundu S, Nicolson W, Chung I, Stafford PJ, et al. Regional fractionation and dominant frequency in persistent atrial fibrillation: effects of left atrial ablation and evidence of spatial relationship. Europace 2011;13:1550-1556.

[7] Lin YJ, Tai CT, Kao T, Chang SL, Wongcharoen W, Lo LW, et al. Consistency of complex fractionated atrial electrograms during atrial fibrillation. Heart Rhythm 2008;5:406-412.

[8] Porter M, Spear W, Akar JG, Helms R, Brysiewicz N, Santucci P, et al. Prospective study of atrial fibrillation termination during ablation guided by automated detection of fractionated electrograms. J Cardiovasc Electrophysiol 2008;19:613-620.

[9] Landis JR, Koch GG. The measurement of observer agreement for categorical data. Biometrics 1977;33:159-174.

[10] Lake DE, Richman JS, Griffin MP, Moorman JR. Sample entropy analysis of neonatal heart rate variability. American journal of physiology Regulatory, integrative and comparative physiology 2002;283:R789-797.

[11] Oakes RS, Badger TJ, Kholmovski EG, Akoum N, Burgon NS, Fish EN, et al. Detection and quantification of left atrial structural remodeling with delayed-enhancement magnetic resonance imaging in patients with atrial fibrillation. Circulation 2009;119:1758-1767.

[12] Sanders P, Berenfeld O, Hocini M, Jais P, Vaidyanathan R, Hsu LF, et al. Spectral analysis identifies sites of high-frequency activity maintaining atrial fibrillation in humans. Circulation 2005;112:789-797.

[13] Everett THt, Moorman JR, Kok LC, Akar JG, Haines DE. Assessment of global atrial fibrillation organization to optimize timing of atrial defibrillation. Circulation 2001;103:2857-2861.